Irradiation effect on deuterium behavior in low dose HFIR neutron-irradiated tungsten

Masashi Shimada¹, G Cao², T Otsuka³, M Hara⁴, M Kobayashi⁵, Y Oya⁵ and Y Hatano⁴

Email address: Masashi.Shimada@inl.gov

PACS: 28.50.Dr, 52.40.Hf, 52.55.Pi, 61.80.Hg, 61.82.Bg, 61.80.Jh

Submitted to IOP Nuclear Fusion

Abstract. Tungsten samples were irradiated by neutrons in the High Flux Isotope Reactor, Oak Ridge National Laboratory at reactor coolant temperature 50-70°C to low displacement damage of 0.025 and 0.3 dpa under the framework of the US-Japan TITAN program (2007-2013). After cooling down, the HFIR neutron-irradiated tungsten samples were exposed to deuterium plasmas in the Tritium Plasma Experiment, Idaho National Laboratory at 100, 200 and 500 °C twice at the ion fluence of 5x10²⁵ m⁻² to reach a total ion fluence of 1x10²⁶ m⁻² in order to investigate the near surface deuterium retention and saturation via nuclear reaction analysis. Final thermal desorption spectroscopy was performed to elucidate irradiation effect on total deuterium retention. Nuclear reaction analysis results showed that the maximum near surface (< 5 micron depth) deuterium concentration increased from 0.5 at. % D/W in 0.025 dpa samples to 0.8 at. % D/W in 0.3 dpa samples. The large discrepancy between the total retention via thermal desorption spectroscopy and the near surface retention via nuclear reaction analysis indicated the deuterium was migrated and trapped in bulk (at least 50 μm depth for 0.025 dpa and 35 μm depth for 0.025 dpa) at 500 °C case even in the relatively low ion fluence of 10²⁶ m⁻².

1. Introduction

Tritium behavior in fusion reactor materials plays a major role in the material selection for future fusion reactors, because tritium retention and permeation determines in-vessel inventory levels and ex-vessel releases in reactor safety assessments [1-3]. Plasma-facing components (PFCs) will be exposed to 14 MeV neutrons from deuterium-tritium fusion reactions. 14 MeV neutrons change the elemental composition via transmutations, and create a high radiation environment inside PFCs, which influence the behavior of hydrogen isotopes in PFCs. Neutron irradiation effects on tritium behavior is one area that has not been well studied in the fusion community due to the difficulty in handling activated material in ion implantation devices and linear plasma devices. Tungsten, a candidate material for the divertor PFC in ITER, is expected to receive a neutron dose of 0.7 displacements per atom (dpa) by the end of operation in

¹ Fusion Safety Program, Idaho National Laboratory, Idaho Falls, ID, U.S.A.

² Department of Engineering Physics, University of Wisconsin-Madison, Madison, WI, U.S.A.

³ Kyushu University, Interdisciplinary Graduate School of Engineering Science, Higashi-ku, Fukuoka, Japan

⁴ Hydrogen Isotope Research Center, University of Toyama, Toyama, Japan

⁵ Radioscience Research Laboratory, Faculty of Science, Shizuoka University, Shizuoka, Japan

ITER [4]. Although tritium inventory in beryllium co-deposit still remains as a major concern for ITER, and that in lose dose (up to 0.7 dpa) neutron-irradiated tungsten needs to be accurately assessed for ITER deuterium-tritium phase of operation. Tungsten and tungsten alloys are a candidate material for the divertor and first wall PFCs in DEMO and future reactor, and the tritium inventory in high dose (>> 1 dpa) neutron-irradiated tungsten / tungsten alloys will be a major concern for DEMO and future fusion reactor. Unavailability of high-flux 14 MeV neutron source (such as IFMIF) remains as a roadblock for assessment of tritium inventory in fusion nuclear environment for DEMO and future fusion.

As the surrogate experiment, the effect of neutron-irradiation damage has been mainly simulated using high-energy ion bombardment [5-9]. While this prior database of results is quite valuable for understanding the behavior of hydrogen isotopes in PFCs, it does not encompass the full range effects that must be considered in a practical fusion environment. The ions are limited in range to only a few μ m into the surface, PKA (the primary knock-on atom) energy (> MeV) from high energy ion-bombardment is much higher than that (< 300 keV) from 14 MeV neutrons, and the displacement rate $(10^{-3}\sim10^{-4}~dpa/sec)$ from high energy ion-bombardment are three to four orders of magnitude higher than that $(10^{-7}\sim10^{-8}~dpa/sec)$ from fission and fusion neutron environments [4]. In addition, the 14 MeV neutrons change the elemental composition via transmutations, and create a high radiation environment inside PFCs, which might have effects on the behavior of tritium in PFCs. Therefore, there still exists large uncertainty about the tritium retention in neutron-radiation damage from the 14 MeV fusion neutrons. For the assessment of tritium inventory, the biggest drawback of these surrogate experiments is the lack of damage creations in the bulk (>> 5 μ m) tungsten, which determines tritium inventory in neutron-irradiated tungsten.

The other approach is to utilize the available fission (mixed spectrum) reactor such as High Flux Isotope Reactor (HFIR) at Oak Ridge National Laboratory or Advanced Test Reactor at Idaho National Laboratory (INL). The fusion neutron spectrum is not mono-energetic 14 MeV, which is created by the deuterium-tritium fusion reaction, but it contains fairly large fraction of the fast (>0.1 MeV) neutrons less than 14 MeV [4]. While fission neutrons alone cannot simulate the effect of 14 MeV neutrons, they can be used to simulate the effects of neutron interactions in the fast neutron energies (up to a few MeV). Fission neutrons with energies greater than 2 MeV are capable of simulating the 2.45 MeV neutrons from the deuterium-deuterium fusion reaction. It is important to note that the displacement rate $(10^{-7} \sim 10^{-8} \text{ dpa/sec})$ in a fission reactor is similar to that of the fusion reactor, and fission reactor is capable of creating damages in the bulk (>> 5 µm) tungsten that determines tritium inventory in neutron-irradiated tungsten. As a result, the utilization of the fission reactor can eliminate uncertainties associated with different displacement rates from using surrogate high-energy ions to simulate neutron damage. In addition, the higher thermal flux fraction in a fission reactor can be used as an advantage to simulate/accelerate transmutations and investigate the transmutations (e.g., rhenium and osmium) and the phase structure changes (e.g., the formation of the rhenium-rich Sigma- and Chi-phases in tungsten) effects on tritium behavior or the irradiation can be carried out with thermal neutron shielding such as cadmium or europium oxide to better represent the fusion neutron energy spectrum. One drawback of neutron-irradiation in tungsten in fission reactor is the lack of hydrogen and helium production. Fission reactors have been widely used to study the irradiation response of structural material development for the fission and fusion materials. Most existing linear plasma devices also lack the ability to handle radioactive materials, making it challenging to study samples irradiated in a fission reactor for plasma wall interaction studies.

INL operates the Tritium Plasma Experiment (TPE), a high-flux linear plasma facility that can handle tritium, beryllium and activated materials. TPE is unique in that it combines four specialized elements: (a) the ability to handle tritium, (b) a divertor-relevant high-flux plasma, (c) the ability to handle radioactive materials, as well as (d) the ability to handle beryllium [10]. Pioneer work of irradiation effects of deuterium behavior in neutron-irradiated tungsten have been carried with the collaborative research under the framework of US-Japan international collaboration, TITAN program [11-18].

In this paper we summarize the material preparation of W samples, the low temperature (50-70 °C) low dose (0.025-0.3 dpa) neutron-irradiation at HFIR, deuterium plasma exposure at TPE, near-surface deuterium retention and deuterium depth profile measurement at University of Wisconsin-Madison, and total deuterium retention measurement at INL. In the section that follows, we describe the theory and calculation of the Tritium Migration Analysis Program (TMAP), and summarize the experimental result of near-surface deuterium retention and deuterium depth profile and total deuterium retention measurement from HFIR neutron-irradiated tungsten. In the final section, we discuss the irradiation effect on deuterium behavior in HFIR neutron-irradiated W and assess the tritium inventory in neutron-irradiated W for ITER deuterium-tritium phase of operation, DEMO, and future fusion reactors.

2. Material preparation and experimental procedures

2.1. Material preparation

The disc-type tungsten samples (φ 6.0 mm x 0.2 mm) were prepared by cutting polycrystalline tungsten rod (99.99 at. % purity, from A.L.M.T. Co., Japan) annealed at 900 °C for 1 hour in a hydrogen atmosphere to relieve internal stresses in the manufacturing process. The detailed impurity content was given in elsewhere [18]. The total concentration impurity was calculated to be 0.05 in at. %. The samples were mechanically polished to a mirror-like finish with abrasive papers and diamond powders (3 and 9 µm), and were given a mirror-like finish with a colloidal silica suspension (40 nm), and then annealed at 900 °C for 0.5 hour in ultra high vacuum (~10⁻⁶ Pa) in order to remove hydrogen contained as an impurity and relieve stress induced by polishing prior to the plasma exposure. The grains are elongated along the direction normal to the plasma-exposed surface, which is similar to ITER grade tungsten for the purpose of minimizing the large blister formation. After the sample preparation at University of Toyama, Japan, the samples were transferred to ORNL for neutron irradiation at HFIR. Due to the limited number of neutron-irradiated samples, the deuterium plasma exposures and nuclear reaction analysis (NRA) measurements were performed twice prior to the final thermal desorption spectroscopy (TDS). Deuterium plasma instead of tritium plasma was used in this study for NRA measurements. Experimental procedures in this research are: (1) neutron-irradiation, (2) 1st deuterium plasma exposure, (3) 1st NRA measurement, (4) 2nd deuterium plasma exposure, (5) 2nd NRA measurement, and (6) TDS measurement.

2.2. Neutron-irradiation at HFIR, ORNL

For the low temperature low dose HFIR irradiation, the tungsten samples were sealed in molybdenum envelopes to prevent cooling water leakage onto the samples but allowing enough heat conduction for the sample to be cooled down to the cooling water temperature, and were irradiated in the perforated aluminum rabbit capsule with neutrons in the HFIR for 33 and 391 hour at the hydraulic tube facility at the coolant temperature of the reactor (50-80 °C). The thermal neutron and fast neutron (>0.1MeV) fluxes at the irradiation location are 2.5×10^{19} , and 8.9×10^{18} m⁻²s⁻¹, respectively. The thermal neutron and fast neutron (>0.1MeV) fluences for 33 hour irradiation are 3.0×10^{24} and 1.1×10^{24} m⁻², respectively. The thermal neutron and fast neutron (>0.1MeV) fluences for 391 hour irradiation are 3.5×10^{25} and 1.3×10^{25} m⁻², respectively. These fast neutron (>0.1MeV) fluences give damage level approximately 0.025 and 0.3 dpa for 33 and 391 hour exposure, respectively.

2.3. Deuterium plasma exposure at TPE, INL

Due to high radioactivity and high dose rate from neutron-irradiated tungsten, the samples were shipped to INL after storage in a water pool and hot cell around 300 and 800 days for 0.025 and 0.3 dpa, respectively. TPE at INL was used to implant low energy (100eV) deuterium ion. In order to investigate the deuterium saturation effect in the radiation damage, TPE exposure were repeated twice at similar plasma condition. Details of the TPE linear plasma device is described elsewhere [10]. Incident ion energy of 100 eV was achieved by adjusting the target bias voltage. The sample temperature was controlled by changing the material (to vary thermal conductivity) and geometry (to vary effective thermal diffusion area) of the heat sinks between the sample and the water-cooled copper plate. The sample temperature was monitored by the ungrounded K-type (chromel-alumel) thermocouple that was attached on the back of the sample. Approximately 15 min is required for the sample temperature to stabilize, and the sample temperature was maintained to the desired temperature (100, 200, and 500 °C) within 10 °C after that. The post-exposure cool-down takes about 10 min to reach room temperature. Since disc-type samples were prepared by cutting polycrystalline tungsten rod, a variation in the sample thickness made it challenging to obtain identical flux and temperature conditions for different thickness sample. The recent report indicated that there exists strong dependence of ion fluence on tritium retention and less dependence of ion flux [19]. Therefore, the ion fluences in each TPE plasma exposure and the cumulative (sum of 1st and 2nd TPE plasma exposures) ion fluences were kept approximately $5x10^{25}$ m⁻², and $1x10^{26}$ m⁻², respectively for each sample as shown in table 1. According to the review of radiation damage recovery in tungsten, the stage III recovery, which is attributed to the migration of mono-vacancies, was observed around 300-400 °C, and the migration energy of mono-vacancy were reported to be approximately 1.7 eV [20]. For the sample exposed at 100 and 200 °C, the sample temperature was kept below the stage III recovery temperature to prevent recovery of neutron-irradiated damage during the deuterium plasma exposure, and the effect of diffusion on the deuterium depth profile is evaluated. For the sample exposed at 500 °C, the sample temperature was above the stage III recovery temperature, and the effects of the stage III recovery on deuterium depth profile is evaluated. The experimental (HFIR irradiation and TPE plasma) conditions are summarized in table 1.

2.4. Near-surface deuterium retention and deuterium depth profile measurement by nuclear reaction analysis (NRA) at University of Wisconsin-Madison

The deuterium depth profiles were measured by the NRA technique with 3.5 MeV 3 He ion beam at the University of Wisconsin-Madison. A 3.5 MeV 3 He beam was carried out to measure the deuteron retention and depth profile using $D(^3$ He,p) 4 He nuclear reaction at the Ion Beam Laboratory at University of Wisconsin-Madison. The 3 He beam was bombarded normal to the tungsten sample and the proton signal was detected with a deep depletion depth (2000 μ m) silicon detector at 135° detection angle. A 10 μ m thick Ni foil was used to block 4 He particles [12]. The SIMNRA program was used to obtain the depth profile up to 5 μ m [21].

2.5. Total deuterium retention measurement by thermal desorption spectroscopy (TDS) at INL

These processes of deuterium plasma exposure and deuterium depth profile measurement were repeated twice to investigate the deuterium saturation effect near surface. The total deuterium retentions were measured by the TDS. The temperature ramp rate was adjusted to 0.167 °C s⁻¹ (10 °C min⁻¹) and maximum temperature was 900 °C. The maximum temperature was chosen not to exceed the stress-relieved and annealed temperatures. Details of the analysis are described elsewhere [10-13]. The stage V recovery, which is attributed to the migration of large clusters, was observed around 800-1000 °C, and the migration energy of the corresponding large cluster were not yet reported [21]. Due to the transfer and handling of radioactive materials, the time interval between the 1st plasma exposure at TPE and the final TDS were approximately 600 and 400 days for 0.025 dpa (Sample ID: Y102, Y103, and Y105) and 0.3 dpa (Sample ID: Y107 and Y112) samples respectively, whereas NRA was carried out 30-60 days after each deuterium plasma exposures.

3. Modeling

TMAP (Tritium Migration Analysis Program) was developed by fusion safety program, INL in 1980's to dynamically analyze dissolved gas movement through structure, between structures and adjoining enclosures, and among enclosures. Historically, it was initiated to assist in evaluation of tritium losses from fusion reactor systems during normal and off-normal/accident conditions for safety analysis. However, it became evident that TMAP has application to a much wider variety of problems, and has been widely used in the PFC community to help understand hydrogen isotope behavior in the PFCs [22-25]. TMAP incorporates a one-dimensional diffusion capability that determines the thermal response of structures, solves equations for solute atom movement through surfaces and in bulk materials, and also includes zero-dimensional equation for flows between and chemical reactions within defined control volumes. TMAP calculates the time-dependent responses of a system of solid structures (may be a layered composite), and a related system of gas-filled volumes or enclosures, with respect to: (1) Movement of solute species across structure surfaces. This movement may be governed by dissociation/recombination or by a solution law, such as Sieverts' or Henry's, or inhibited from crossing the surface, (2) Movement by Fick's-law diffusion in the bulk of a structure with optional trapping within a structure, (3) Thermal response of structures to applied heat or boundary temperature loadings conditions, (4) Chemical reactions within enclosures, and (5) Convective flow between enclosures.

The version 4 (TMAP4) was underwent rigorous quality certification to Quality Assurance Level A [26]. The version 7 (TMAP7) used in our previous studies limits the maximum number of trap site to three [11-13, 27], and we simulated the experimental result of 0.025 dpa at 200C by combining two TMAP7 spectra with three trap sites (total of six trap sites) due to the maximum trap site limitation in TMAP7 in our previous study [13]. A recent extension of the TMAP trap site model was successfully carried out in the version 4 (TMAP4) to include as many traps as required by the user to simulate retention of tritium in neutron damaged tungsten material [28]. The recently modified version of TMAP4 was used in this research.

For mass transport properties of deuterium in tungsten, we chose the hydrogen diffusivity formula by Frauenfelder [29] (corrected for deuterium) as the review paper by Causey [30] suggested (D=2.9x10⁻⁷exp(-0.39eV/kT) [m²/s]) in this simulation. Recombination coefficients vary by several orders of magnitude in the literature, and the recombination coefficient formula by Anderl at al [25] $(K_r=3.2\times10^{-15} \exp(-1.16\text{eV/kT}) \text{ [m}^4/\text{s]})$ was used in previous studies [11-12]. This recombination coefficient is high enough to treat surface deuterium concentration to zero; therefore, we treat the surface deuterium concentration to be zero as a boundary condition in this simulation as suggested by Causey et.al.[22-24]. In our previous studies, plasma exposure phase was not simulated for simplicity and near surface (< 5 µm) deuterium depth profiles and detrapping energies of three trap sites were adjusted to fit the experimental TDS spectra based upon the assumption that deuterium were trapped only in near surface (< 5 μm) [11-13]. In the Results section, we found experimentally that this assumption did not hold true for 500 °C case, which showed deep migration (>> 10 um) of deuterium. Due to unavailability of deuterium depth profile diagnostic beyond the detection limit (~ 5 µm with 3.5 MeV ³He) of NRA technique. deuterium migration to bulk tungsten can only be estimated by modeling or simulation such as In this study the enhanced diffusion zone (EDZ) model that Venhaus and Causey simulated tritium plasma implantation was used to simulate two plasma exposure phases and thermal desorption phase and accurately elucidate deuterium behavior in neutron-irradiated tungsten [23-24]. The motivation for the use of this EDZ in implantation zone (<10 nm for incidence energy 100 eV) is based on that extremely high concentration condition of deuterium solution atom in this narrow implantation zone, which can become several orders of magnitude larger than the solution concentration calculated from solubility law, has significant impact on deuterium behavior. It is known that deuterium favors precipitation under extremely high hydrogen solution concentration and forms deuterium bubble in tungsten [31]. One of the possible mechanisms for the enhanced diffusion in implantation zone is the connection of these hydrogen bubbles, creating diffusion path of deuterium atom to the surface and increasing reflux of deuterium molecule from surface. Venhaus and Causey adjusted the diffusivity in the EDZ from $5.0x10^{-10}$ to $2.0x10^{-9}$ m²/s to fit experimental data. In this paper we utilized the EDZ in ion implantation zone (<10 nm), and varies the deuterium diffusivity in the similar range from 0.9×10^{-10} to 5.0×10^{-10} m²/s to fit experimental data. Deuterium implantation profile (100 eV D⁺ in W) obtained from SRIM was used for this simulation [32]. Hydrogen diffusivity formula (corrected for deuterium) by Frauenfelder was used in normal diffusion zone (NDZ), which is beyond 10 nm from surface.

From the literature of the detrapping energy in tungsten [33-35], the low-energy (0.8-1.1 eV) trap is associated deuterium atoms trapping with impurities or dislocations, the 1.3-1.5 eV trap is associated with deuterium atoms trapping at vacancies in tungsten and deuterium

molecules desorbed from voids, and the high-energy (1.7-2.1 eV) trap is associated with dissociation and release of deuterium atoms decorating a void. Uniform distribution of empty traps with user specified concentration is introduced first, and two deuterium plasma exposures are simulated with similar deuterium ion flux and temperature profiles obtained experimentally to investigate deuterium behavior (e.g. how deep deuterium atoms migrate and trap) in tungsten. Then, the thermal desorption phase were simulated with the ramp rate (0.167 °C s⁻¹ = 10 °C min⁻¹) and the maximum temperature of 900 °C.

There exist three types of fitting parameters in TMAP modeling in this study. The diffusivity in the EDZ determines deuterium solution concentration penetrating to the NDZ, therefore it governs how deep deuterium atom can migrate with given trap concentration and detrapping energy. Effective diffusivity decreases as the trap concentration and detrapping energy increase. In general, the first fitting parameter, detrapping energy, can be determined by the TDS peak positions, and the second fitting parameter, trap concentration, can be obtained by the maximum deuterium flux (peak height) of TDS peak. Uniform trap concentration throughout sample thickness was used for simplicity and due to unavailability of deuterium depth profile diagnostic in bulk W ($> 5 \mu m$). The third fitting parameter, diffusivity in the EDZ, can be acquired from the shape (width) of TDS peak.

4. Results

Experimental procedures in this research are: (1) neutron-irradiation, (2) 1st deuterium plasma exposure, (3) 1st NRA measurement, (4) 2nd deuterium plasma exposure, (5) 2nd NRA measurement, and (6) TDS measurement. Section 4.1 discusses the results from (3) 1st NRA measurement and (5) 2nd NRA measurement, and Section 4.2 discusses the results from (6) TDS measurement. Then Section 4.3 compares near-surface deuterium retention with total deuterium retention. Section 4.4 describes the TMAP modeling results of experimental TDS spectra.

4.1 Near-surface deuterium depth profile from neutron-irradiated tungsten

Figure 1 shows the 1st NRA near-surface (0-5 μm) deuterium depth profiles of 0.025, and 0.3 dpa neutron-irradiated tungsten samples exposed to the ion fluence of 5x10²⁵ m⁻² at (a) 200 °C and (b) 500 °C along with the non-irradiated (0 dpa) tungsten samples, and the 2nd NRA nearsurface (0-5 µm) deuterium depth profiles of 0.025, and 0.3 dpa neutron-irradiated tungsten samples exposed to the total ion fluence of 1×10^{26} m⁻² at (c) 200 °C and (d) 500 °C along with the non-irradiated (0 dpa) tungsten samples. For 200 °C, 1st NRA (figure 1a), the deuterium was observed to be migrated to a depth of approximately 3 µm, and the migration depth deepened as the neutron dose increase from 0.025 to 0.3 dpa. The maximum deuterium concentration increased from 0.4 at. % at 0.025 dpa to 0.8 at. % at 0.3 dpa. For 500 °C, 1st NRA (figure 1b), the deuterium was observed to be migrated to beyond the NRA detection range of 5 µm for neutronirradiated tungsten, while deuterium concentration level was below the NRA detection limit of 0.005 at % for non-irradiated tungsten (0 dpa). The maximum deuterium concentration increased from 0.2 at. % at 0.025 dpa to 0.4 at. % at 0.3 dpa. Figure 1b also shows the trends of surface desorption during the cooling down phase. For 200 °C, 2nd NRA (figure 1c), the deuterium was migrated further to the NRA detection range of 5 µm, and the migration depth deepened as the neutron dose increase from 0.025 to 0.3 dpa. The maximum deuterium concentration increased from 0.5 at. % at 0.025 dpa to 1.0 at. % at 0.3 dpa, which were increased from figure 1a. For 500 $^{\circ}$ C, 2^{nd} NRA (figure 1d), the deuterium was observed to be migrated to beyond the NRA detection range of 5 μ m for neutron-irradiated tungsten, and deuterium concentration level increased to 0.05 at. % for non-irradiated tungsten (0 dpa). The maximum deuterium concentration increased from 0.2 at. % at 0.025 dpa to 0.3 at. % at 0.3 dpa, which were similar to Figure 1b. The Figure 2b also shows the trend of surface desorption during the cooling down phase.

Near-surface deuterium depth profile via NRA (figures 1) showed that the deuterium was migrated to beyond the NRA detection range of 5 µm for neutron-irradiated tungsten, and the maximum deuterium concentration increased approximately a factor of 2 (from 0.5 to 1.0 at. %) in the order of magnitude increase in neutron dose (from 0.025 to 0.3 dpa). The observation of surface desorption during the cooling down phase suggests that the detrapping energy of predominant traps at near surface (5 µm) might be relatively low energy. Figure 2 shows the maximum deuterium concentration with damage level. For 200 °C case, the maximum deuterium concentration increased 20 % from 0.8 at. % at for 1st NRA to 1.0 at. % for 2nd NRA. For 500 °C case, the maximum deuterium concentration decreased 25 % from 0.4 at. % at for 1st NRA to 0.3 at. % for 2nd NRA. This indicated that the trapping site can be annealed during 500 °C plasma exposure or detrapping occurs at 500°C, not filling out traps completely. Further investigation is required to confirm this annealing phenomenon at 500 °C.

4.2 Thermal desorption spectra from neutron-irradiated tungsten

After two deuterium plasma exposures at TPE and two NRA measurements at UW-Madison, the final TDS were performed at INL. Figure 3 shows the thermal desorption spectra of 0.025, and 0.3 dpa neutron-irradiated tungsten samples exposed to the total ion fluence of $1x10^{26}$ m⁻² at (a) 200 °C and (b) 500 °C along with the non-irradiated (0 dpa) tungsten sample.

For 200 °C case, Figure 3a shows similar profiles with two distinctive peaks: a low temperature peak located around 250-350 °C, and a high temperature peak located around 500-600 °C. The maximum deuterium desorption flux increased from 0.025 dpa to 0.3 dpa. Non-irradiated (0 dpa) tungsten sample shows one low temperature peak located around 350-450 °C. For 500 °C case, Figure 3b shows similar profiles with one distinctive peak located different temperature around 750-850 °C for 0.025 dpa and 500-600 °C for 0.3 dpa. It has a shoulder profile around 700 °C for 0.3 dpa. The maximum deuterium desorption flux decreased slightly from 0.025 dpa to 0.3 dpa. Non-irradiated (0 dpa) tungsten sample shows no deuterium retention below the TDS detection limit of 8x10¹⁷ m⁻²s⁻¹.

4.3 Comparison of near-surface deuterium retention and total deuterium retention

Integrating the NRA deuterium concentration profile gives near-surface (0-5 μ m) deuterium retention. Figure 4 summarizes the near-surface (0-5 μ m) deuterium retention via NRA and the total deuterium retention via TDS at three different plasma exposure temperatures (100, 200, and 500 °C). Figure 4a shows the near-surface (0-5 μ m) deuterium retention at three different plasma exposure temperatures (100, 200, and 500 °C). At 100 °C, the near-surface deuterium retention from 0.025 dpa neutron-irradiated W is $3x10^{20}$ m⁻², which is similar to that of non-irradiated tungsten (0 dpa). At 200 °C, the near-surface deuterium retention increased from $1.5x10^{21}$ m⁻² at 0.025 dpa to $3.0x10^{21}$ m⁻² at 0.3 dpa. At 500 °C, the near-surface deuterium

retention increased from 6.0×10^{20} m⁻² at 0.025 dpa to 9.0×10^{20} m⁻² at 0.3 dpa. Figure 4b shows the total deuterium retention at three different plasma exposure temperatures (100, 200, and 500 °C). At 100 °C, the total deuterium retention from 0.025 dpa neutron-irradiated tungsten is 1.5×10^{20} m⁻². At 200 °C, the total deuterium retention increased from 1.2×10^{21} m⁻² at 0.025 dpa, which is similar to that of non-irradiated tungsten (0 dpa), to 5.0×10^{21} m⁻² at 0.3 dpa. At 500 °C, the total deuterium retention was similar at 7.0×10^{22} m⁻² for 0.025 dpa and 0.3 dpa, while that of non-irradiated tungsten (0 dpa) is close to the TDS detection limit of 1.0×10^{20} m⁻².

Large discrepancies between near-surface (0-5 μ m) deuterium retention and total deuterium retention were observed for 500 °C, and it indicated that deuterium was migrated deeply into the bulk in the ion fluence of 10^{26} m⁻² at 500 °C plasma exposed temperature. The near-surface retention at 500 °C were $6.0x10^{20}$ and $9.0x10^{20}$ m⁻² for 0.025 dpa and 0.3 dpa, respectively, whereas the total retention at 500 °C were $6.0x10^{21}$ m⁻² for both 0.025 dpa and 0.3 dpa. The ratio of near-surface retentions to total retentions were a factor of 10 and 7 for 0.025 and 0.3 dpa, respectively, indicating that deuterium was migrated and trapped up to 50 and 35 μ m from the plasma exposed surface for 0.025 and 0.3 dpa, respectively when uniform deuterium concentration is assumed.

4.4 TMAP modeling of experimental TDS spectra

As described in Section 3, both two plasma exposure phases and thermal desorption phase were simulated with the EDZ model in TMAP4 to accurately elucidate deuterium behavior in neutron-irradiated tungsten. Figure 5 shows the deuterium ion implantation profile used in the TMAP simulation along with the profile obtained by SRIM code for 100 eV deuterium ion in tungsten [32]. Deuterium ions were introduced at a rate of the measured deuterium ion flux with the reflection coefficient of approximately 0.5. Deuterium diffusivity were adjusted from 0.9x10⁻¹⁰ to 5.0x10⁻¹⁰ m²/s in the EDZ, which is <10 nm from surface, to fit experimental data, whereas hydrogen diffusivity formula (corrected for deuterium) by Frauenfelder was used in normal diffusion zone (>10 nm). This modified TMAP modeling improves on treating deuterium trapping in bulk, but it's not suitable to explain the enhanced trapping in near surface due to ion-induced damages. As shown in figure 3b, we can assume that there is no near surface trapping for 500 °C exposure sample since D retention was near detection limit for 0 dpa case. Further modification is required to properly simulate near surface trapping at low exposure temperature such as 200 °C.

Figure 6 shows TMAP4 modeling of thermal desorption spectra of 0.025, and 0.3 dpa neutron-irradiated tungsten samples exposed to the total ion fluence of 1x10²⁶ m⁻² at (a) 200 °C and (b) 500 °C. In all cases, TMAP was capable of predicting TDS spectra with reasonable trap concentration, detrapping energy, and diffusivity in the EDZ except for the high-energy tail of TDS spectra in figure 6a. Figure 7 shows detrapping energy and trap concentration of trap sites obtained from TMAP modeling on experimental TDS spectra of 0.025, and 0.3 dpa neutron-irradiated W samples exposed to the total ion fluence of 1x10²⁶ m⁻² at 200 °C and 500 °C. There exists roughly two TDS peaks for 200 °C (low temperature peak and high temperature peak), whereas there is only one TDS peak for 500 °C (high temperature peak). Figure 7 shows how trap concentration and detrapping energy were changed as the displacement damage increase from 0.025 to 0.3 dpa. For 0.025 dpa, 200 °C case, approximately two orders of magnitude lower trap concentrations (~ 5.0x10⁻⁵ T/W) were obtained from both low and high temperature peaks

than the NRA results ($\sim 5.0 \times 10^{-3}$ D/W) in Figure 2. In addition two orders of magnitude increase in trap concentrations were obtained from 5.0×10^{-5} to 5.0×10^{-3} T/W for 200 °C case as the displace damage increase only one order of magnitude from 0.025 to 0.3 dpa. Therefore, there still exists large discrepancy between experimental results and TMAP modeling at 200 °C case. Further modification is required to properly simulate near surface trapping due to ion-induced damages at 200 °C. However, this modified TMAP modeling should properly predict deuterium behavior in bulk W for 500°C case. One order of magnitude increase in trap concentrations was obtained from 1.5x10⁻³ to 1.5x10⁻² T/W for 500 °C case and detrapping energy decreases from 1.75 to 1.4 eV as the displace damage increase from 0.025 to 0.3 dpa. The mechanism of the shift of detrapping energy is unknown at this moment, and more experimental data is required to confirm this shift. Figure 8 shows deuterium depth profile obtained from TMAP modeling on experimental TDS spectra of 0.025, and 0.3 dpa neutron-irradiated tungsten samples exposed to the total ion fluence of 1x10²⁶ m⁻² at 200 °C and 500 °C. Fore 200 °C case, two orders of magnitude increase in maximum deuterium concentrations were obtained from 1.0x10⁻⁴ to 1.0x10⁻² D/W as the displacement damage increase only one order of magnitude from 0.025 to 0.3 dpa. Deep penetration and trapping (> 100 μm) of deuterium was obtained at 0.025 dpa 200 °C case, but this is due to unavailability of near surface trapping simulation capability in this simulation. For 500 °C case, a factor of 5 increase in maximum deuterium concentration was obtained from 1.0×10^{-3} to 5.0×10^{-3} D/W as the displacement damage increase from 0.025 to 0.3dpa. The maximum deuterium concentration via NRA was in the similar concentration (from 2.0×10^{-3} to 3.0×10^{-3} D/W) as shown in figures 1b and 2. For the sample exposed at 500 °C, deuterium atom were migrated and trapped up to 100 µm and 40 µm from the plasma exposed surface for 0.025 and 0.3 dpa, respectively. This is very similar to the experimental observation of up to 50 and 35 µm from the plasma-exposed surface for 0.025 and 0.3 dpa. This agreement between experimental observation and TMAP modeling confirms that the modified TMAP modeling is capable of properly simulating deuterium behavior in bulk at high temperature, but it requires further modification to accurately explain the near surface trapping due to ion-induced damages at low temperature.

5. Discussion

There exist lack of microstructure and defect recovery studies of neutron-induced radiation damages in tungsten, making it challenging fusion community to accurately understand radiation damage effects on hydrogen isotope behavior. Microstructure of molybdenum, high Z bcc metal, was extensively studied via transmission electron microscopy (TEM) and positron annihilation spectroscopy (PAS) and it helps understand radiation damage mechanism in W [36]. The irradiation was carried out at the identical irradiation location (hydraulic tube facility) in HFIR at the identical temperature (reactor coolant temperature), and this study provides data from wider displacement damage range from 0.000072 to 0.28 dpa. The TEM and PAS observation showed that low dose HFIR neutron-irradiation produced predominantly mono-vacancy at low temperature in molybdenum below 0.3 dpa, and the number density of mono-vacancy saturate to around 10^{24} m⁻³ from 0.01 dpa to 0.3 dpa whereas the number density of vacancy cluster (3 and 10 vacancies) keeps increasing approximately with a square root of displacement damage (~dpa^{0.5}). Though the number density of large (>50 vacancy) vacancy cluster is two orders of magnitude lower than those of vacancy clusters (3 and 10 vacancies), it increases linearly with

displacement damage (~ dpa¹). The mean diameter of larger clusters was calculated to be approximately 0.5-0.6 nm in molybdenum, and does not depend on displacement damage. The stage III recovery, which is attributed to the migration of mono-vacancies, was observed around 300-400 °C, and the migration energy of mono-vacancy were reported to be approximately 1.7 eV [20]. Assuming that the radiation damage in tungsten is similar to in molybdenum, low dose HFIR neutron-irradiation creates predominantly mono-vacancy at low temperature in tungsten. For the sample exposed at 100 and 200 °C, which is below the stage III recovery temperature, mono-vacancy is not capable of migrating to form larger vacancy cluster. Therefore, monovacancy should be the predominant radiation damage in the sample exposed to plasma at 100 and 200 °C, and the number density of mono-vacancy should be similar from 0.025 dpa to 0.3 dpa as it saturate above 0.01 dpa. However, displacement damage dependence on deuterium retention and trap concentration in both peaks were observed at 200 °C as shown in figure 3, suggesting mono-vacancy might not be predominant trapping mechanism in HFIR neutron-irradiated tungsten at 200 °C. For the sample exposed at 500 °C, which is above the stage III recovery temperature, mono-vacancy starts migrating to form larger vacancy clusters. Figures 7 shows the linear increase in trap concentration from 0.025 dpa to 0.3 dpa, indicating predominant trapping mechanism is large (>50 vacancy) vacancy cluster for the sample exposed to plasma at 500 °C. Figures 7 shows also the decrease in detrapping energy (from 1.75 to 1.4 eV) from 0.025 dpa to 0.3 dpa, suggesting microstructural change due to agglomeration of large (>50 vacancy) vacancy clusters decreases detrapping energy. Further investigation is necessary to conclude this assumption. Both experimental evidence in figure 4 and numerical suggestion in figure 7 confirmed that deuterium can be migrated and trapped at deep (>> 10 µm) in neutron-irradiated tungsten in the sample exposed to plasma at 500 °C. This can become serious safety issue when tungsten is used in DEMO, in which the first wall and divertor expect to be operated at high temperature (> 500 °C).

6. Conclusions

Radiation damage created by HFIR neutron in the bulk tungsten acts as trapping sites for deuterium atoms. HFIR neutron-irradiated tungsten samples were exposed to deuterium plasmas in the TPE at 100, 200 and 500 °C twice at the ion fluence of 5x10²⁵ m⁻² to reach a total ion fluence of 1x10²⁶ m⁻² aiming at investigating the near surface deuterium retention and saturation via NRA. NRA measurements showed further migration of deuterium atom from the 1st NRA measurement after 5x10²⁵ m⁻² ion fluence to the 2nd NRA measurement after 1x10²⁶ m⁻² ion fluence at 200 °C case. Final TDS was performed to elucidate irradiation effect on total deuterium retention. Near-surface deuterium retention results via NRA show the maximum deuterium concentration was at 1.0 at. % and 0.4 at. % at 200 °C and 500 °C, respectively. The near-surface retention at 500 °C were 6.0×10^{20} and 9.0×10^{20} m⁻² for 0.025 dpa and 0.3 dpa, respectively, whereas the total retention at 500 °C were 6.0x10²¹ m⁻² for both 0.025 dpa and 0.3 dpa. The ratio of near-surface retentions to total retentions were a factor of 10 and 7 for 0.025 and 0.3 dpa, respectively, indicating that deuterium was migrated and trapped up to 50 and 35 μm for 0.025 and 0.3 dpa, respectively when uniform deuterium concentration is assumed. Numerical study of TMAP with the EDZ confirmed that deuterium can be migrated and trapped at bulk tungsten (50 and 35 µm from the plasma exposed surface) in the low temperature (50-70 °C) low dose (0.025-0.3 dpa) neutron-irradiation tungsten. This collaborative research under US-Japan TITAN program demonstrated experimentally and numerically that deuterium is migrated and trapped deep at deep (>> $10 \mu m$) in neutron-irradiated tungsten in the sample exposed to plasma at 500° C. This finding can lead to serious safety issue that tritium can be migrated and trapping in bulk tungsten in DEMO, in which the first wall and divertor expect to be operated at high temperature (> 500° C), therefore; further research is still required experimentally and numerically to reveal the underlying physics of tritium behavior in neutron-irradiated tungsten and to find the mitigation method of deep migration and trapping.

Acknowledgement

This work was prepared for the U.S. Department of Energy, Office of Fusion Energy Sciences; under the DOE Idaho Field Office contract number DE-AC07-05ID14517. This work was performed under US-Japan collaborative research project, TITAN.

References

- [1] Taylor N, Baker D, Ciattaglia S, Cortes P, Elbez-Uzan J, Iseli M, Reyes S, Rodriguez-Rodrigo L, Rosanvallon S, Topilski L, *Fus. Eng. Des.* **86** (2011) 619
- [2] Taylor N, Ciattaglia S, Cortes P, Iseli M, Rosanvallon S, and Topilski L, Fus. Eng. Des. 87 (2012) 476
- [3] Taylor N, Alejaldre C, and, Cortes P, Fus. Sci. Technol. 64 (2013) 111
- [4] Iida H, Khripunov V, Petrizzi L, and Federici G, 2004 ITER Nuclear Analysis Report G 73 DDD 2 W 0 (2004)
- [5] Wampler W R, and Doerner R P, Nucl. Fusion 49 (2009) 115023
- [6] Tyburska B, Alimov V Kh, Ogorodnikova O V, Schmid D, and Ertl K, *J. Nucl. Mater.* **395** (2009) 1150
- [7] Fukumoto M, Kashiwagi H, Ohtsuka Y, Ueda Y, Nobuta Y, Yagyu J, Arai T, Taniguchi M, Inoue T, and Sakamoto K, *J. Nucl. Mater.* **386–388** (2009) 768
- [8] Fukumoto M, Kashiwagi H, Ohtsuka Y, Ueda Y, Taniguchi M, Inoue T, Sakamoto K, Yagyu J, Arai T, Takagi I, and Kawamura T, *J. Nucl. Mater.* **390-391** (2009) 572
- [9] Wright G M, Mayer M, Ertl K, de Saint-Aubin G, and Rapp J, *Nucl. Fusion* **50** (2010) 075006
- [10] Shimada M, Kolasinski R D, Sharpe J P, and Causey R A, Rev. Sci. Instru. 82 (2011) 083503
- [11] Shimada M, Hatano Y, Calderoni P, Oda T, Oya Y, Sokolov M, Zhang K, Cao G, Kolasinski R D, and Sharpe J P, *J. Nucl. Mater.* **415** (2011) S667
- [12] Shimada M, Cao G, Hatano Y, Oda T, Oya Y, Hara M, and Calderoni P, *Phys. Scr.* **T145** (2011) 014051
- [13] Shimada M, Hatano Y, Oya Y, Oda T, Hara M, Cao G, Kobayashi M, Sokolov M, Watanabe H, Tyburska-Puschel B, Ueda Y, Calderoni P, and Okuno K, *Fus. Eng. Des.* **87** (2012) 1166
- [14] Oda T, Shimada M, Zhang K, Calderoni P, Oya Y, Sokolov M, Kolasinski R D, Sharpe J P, and Hatano Y, Fus. Sci. Technol. **60** (2011) 1455
- [15] Oya Y, Shimada M, Oda T, Hara M, Hatano Y, Calderoni P, and Okuno K, *Phys. Scr.* **T145** (2011) 014050
- [16] Hatano Y, Shimada M, Oya Y, Cao G, Kobayashi M, Hara M, Merrill B J, Okuno K, Sokolov M, and Katoh Y, *Mater. Trans.* **54** (2013) 437
- [17] Hatano Y, Shimada M, Alimov V Kh, Shi J, Hara M, Nozaki T, Oya Y, Kobayashi M, Okuno K, Oda T, Cao G, Yoshida N, Futagami N, Sugiyama K, Roth J, Tyburska-Püschel B, Dorner J, Takagi I, Hatakeyama M, Kurishita H, and Sokolov M A, *J. Nucl. Mater.* **438** (2013) S114
- [18] Hatano Y, Shimada M, Otsuka T, Oya Y, Alimov V Kh, Hara M, Shi J, Kobayashi M, Oda T, Cao G, Okuno K, Tanaka T, Sugiyama K, Roth J, Tyburska-Püschel B, Dorner J, Yoshida N, Futagami N, Watanabe H, Hatakeyama M, Kurishita H, Sokolov M A, and Katoh Y, Nucl. Fusion 53 (2013) 073006
- [19] Lipschultz B, Roth J, Davis J W, Doerner R P, Haasz A A, Kalenbach A, Kirschner A, Kolasinski R D, Loarte A, Philipps V, Schmid K, Wampler W R, Wright G M, and Whyte D G, "An assessment of the current data affecting tritium retention and its use to project towards T retention in ITER", MIT Report PSFC/RR-10-4, 2010

- [20] Schultz H, "The Landolt-Börnstein Database (http://www.springermaterials.com)" volume III/25 "Atomic Defects in Metals" (Springer Materials 1991), ed Ullmaier H, section 2.2.3. DOI: 10.1007/10011948 54
- [21] Mayer M, "SIMNRA User's Guide", Tech. Rep. IPP 9/113, (IPP Garching, 1997) http://www.rzg.mpg.de/~mam.
- [22] Causey R A, Wilson K, Venhaus T, and Wampler W R, J. Nucl. Mater. 266-269 (1999) 467-471
- [23] Venhaus T, Causey R A, Doerner R P, and Abeln T, J. Nucl. Mater. 290-293 (2001) 505-508
- [24] Venhaus T, and Causey R A, Fusion Technology, 39 (2001), 868-873
- [25] Anderl R A, Holland D F, Longhurst G R, Pawelko R J, Trybus C L, and Sellers C H, Fus. Technol. 21 (1992) 745
- [26] Longhurst G R, Holland D F, Jones J L, and Merrill B J, "TMAP4 User's Manual", Idaho National Laboratory, EGG-FSP-10315 (1992)
- [27] Longhurst G R, "TMAP7: Tritium Migration Analysis Program," User Manual, Idaho National Laboratory, INEEL/EXT-04–02352, Rev. 2 (2008)
- [28] Merrill B J, Shimada M, and Humrickhouse P W, J. Plasm. Fus. Res. SERIES, 10 (2013) 71
- [29] Frauenfelder R, J. Vac. Sci. Technol. 6 (1969) 388
- [30] Causey R A, J. Nucl. Mater. 300 (2002) 91
- [31] R.D. Kolasinski, D.F. Cowgill, D.C. Donovan, M. Shimada, and W.R. Wampler, J. Nucl. Mater. 438 (2013) S1019
- [32] Stopping and Range of Ions in Matter (SRIM), J.F. Ziegler, http://www.srim.org
- [33] Ogorodnikova O V, Roth J, and Mayer M, J. Appl. Phys. **103** (2008) 034902
- [34] Eleveld H, and van Veen A, J. Nucl. Mater. 191-194 (1992) 433
- [35] Eleveld H, and van Veen A, J. Nucl. Mater. 212-215 (1994) 1421
- [36] Meimei Li, M. Eldrup, T.S. Byun, N. Hashimoto, L.L. Snead, and S.J. Zinkle, J. Nucl. Mater. 376 (2008) 11

Tables

Table 1. The experimental (HFIR irradiation^a and TPE plasma^b) conditions.

Sample ID	Weight [gram]	Sample size ^c (diameter / thickness) [mm]	HFIR irradiation dose [dpa]	TPE exposure temperature [°C]	1st TPE exposure flux [m ⁻² s ⁻¹]	2nd TPE exposure flux [m ⁻² s ⁻¹]	1st TPE exposure fluence [m ⁻²]	2nd TPE exposure fluence [m ⁻²]	Cumulative fluence ^d [m ⁻²]
Y102	0.80	6.0 / 0.15	0.025	100	5.3E+21	5.3E+21	5.0E+25	5.0E+25	1.0E+26
Y103	0.89	6.0 / 0.16	0.025	200	7.0E+21	6.4E+21	5.0E+25	4.6E+25	9.7E+25
Y105	0.83	6.0 / 0.15	0.025	500	7.3E+21	9.3E+21	5.3E+25	6.7E+25	1.2E+26
Y107	0.90	6.0 / 0.17	0.3	200	1.1E+22	1.1E+22	5.0E+25	5.0E+25	1.0E+26
Y112	0.91	6.0 / 0.17	0.3	500	1.1E+22	9.0E+21	5.0E+25	5.0E+25	1.0E+26

^a HFIR irradiation temperature was at the reactor coolant temperature of 50-70 °C

[table width: two columns]

b Incident ion energy was approximately 100 eV for all samples.

c, d Sample thickness varies due to slicing 6 mm diameter tungsten rod. This variation in the sample thickness made it challenging to obtain identical flux and temperature conditions for different thickness sample. The ion fluences in each TPE plasma exposure and the cumulative (sum of 1st and 2nd TPE plasma exposures) ion fluences were kept approximately $5x10^{25}$ m⁻², and $1x10^{26}$ m⁻², respectively for each sample.

Figures

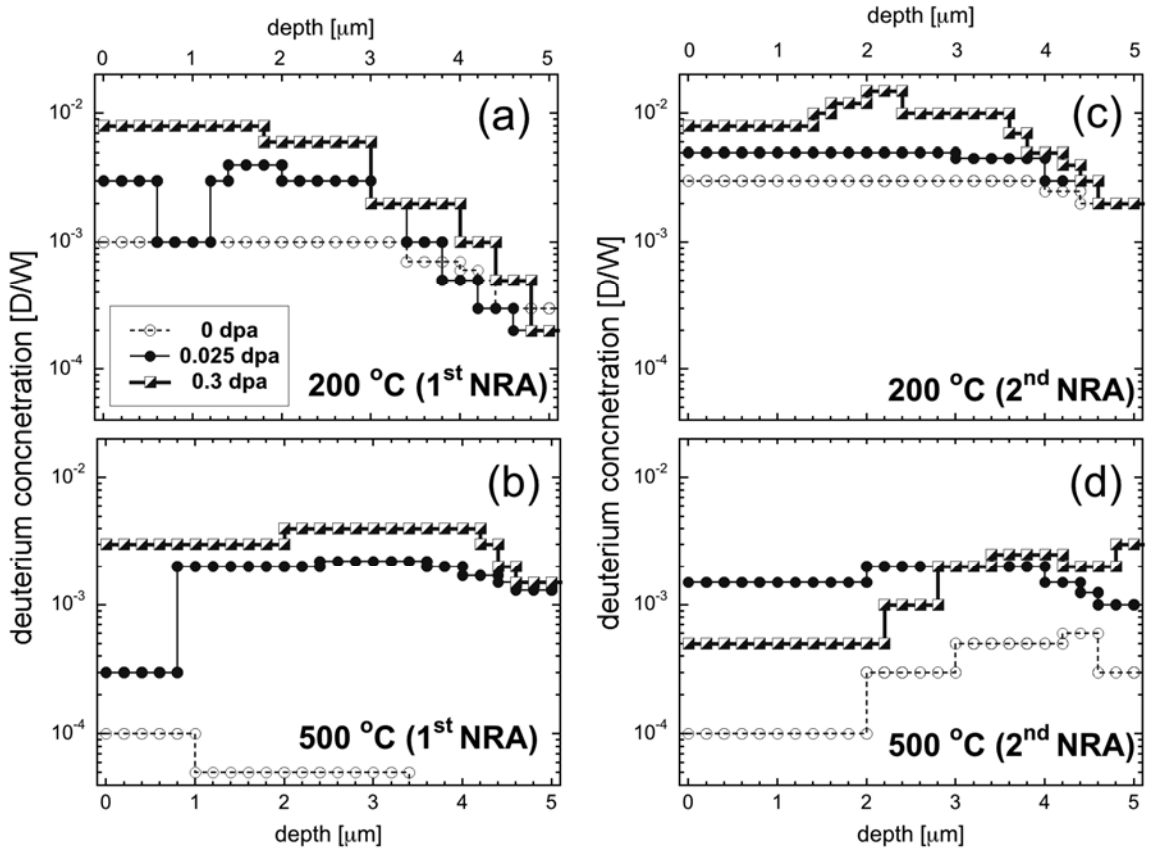


Figure 1. 1st NRA near-surface (0-5 μ m) deuterium depth profiles of 0.025, and 0.3 dpa neutron-irradiated tungsten samples exposed to the ion fluence of $5x10^{25}$ m⁻² at (a) 200 °C and (b) 500 °C along with the non-irradiated (0 dpa) W samples, and 2nd NRA near-surface (0-5 μ m) deuterium depth profiles of 0.025, and 0.3 dpa neutron-irradiated tungsten samples exposed to the total ion fluence of $1x10^{26}$ m⁻² at (c) 200 °C and (d) 500 °C along with the non-irradiated (0 dpa) tungsten samples.

[figure width: two columns, black and white only, filename: "NF MShimada fig1.tif"]

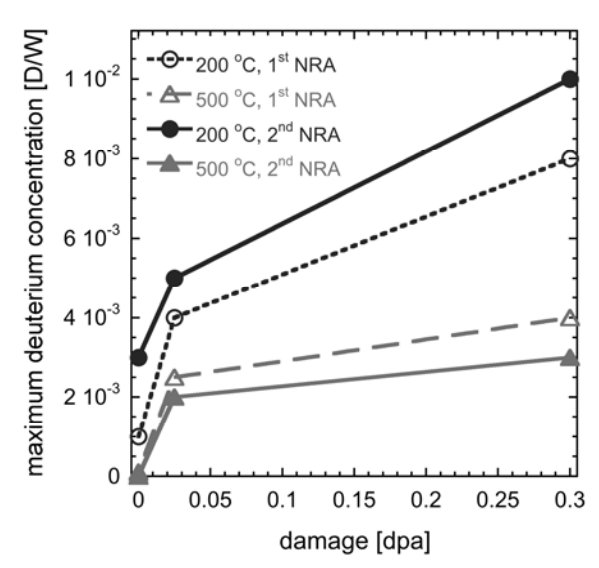


Figure 2. Maximum deuterium concentration with damage level of 0.025, and 0.3 dpa neutron-irradiated tungsten samples exposed at 200 °C and 500 °C along with the non-irradiated (0 dpa) W samples.

[figure width: one column, black and white only, filename: "NF_MShimada_fig2.tif"]

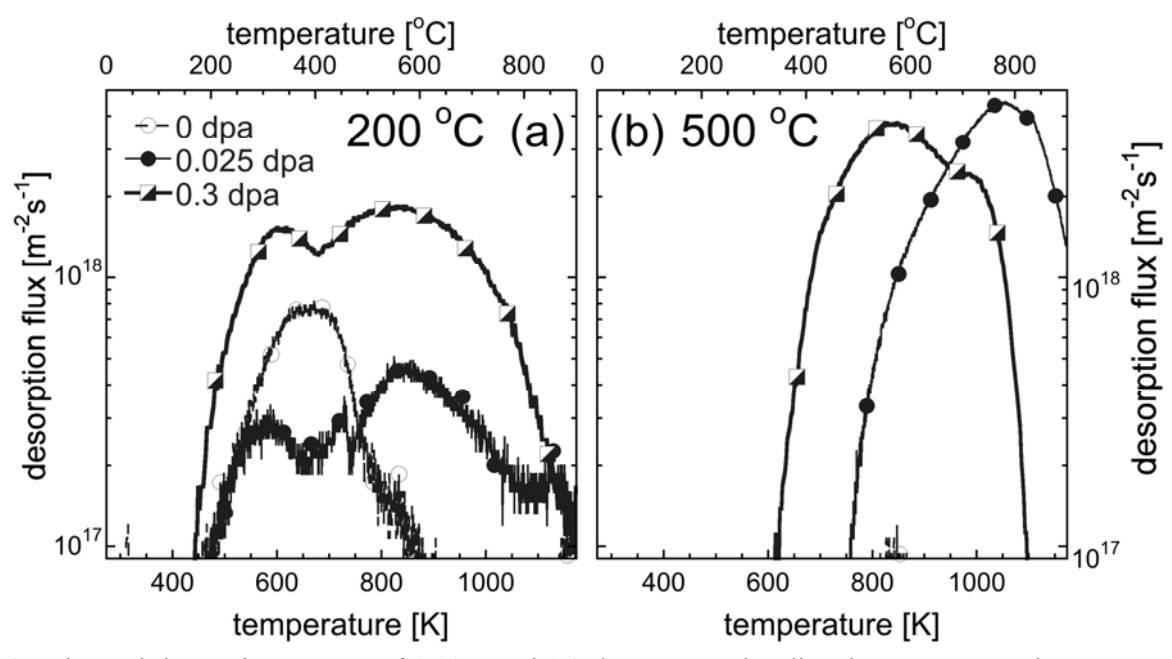


Figure 3. Thermal desorption spectra of 0.025, and 0.3 dpa neutron-irradiated tungsten samples exposed to the total ion fluence of $1x10^{26}$ m⁻² at (a) 200 °C and (b) 500 °C along with the non-irradiated (0 dpa) tungsten sample.

[figure width: two column, black and white only, filename: "NF_MShimada_fig3.tif"]

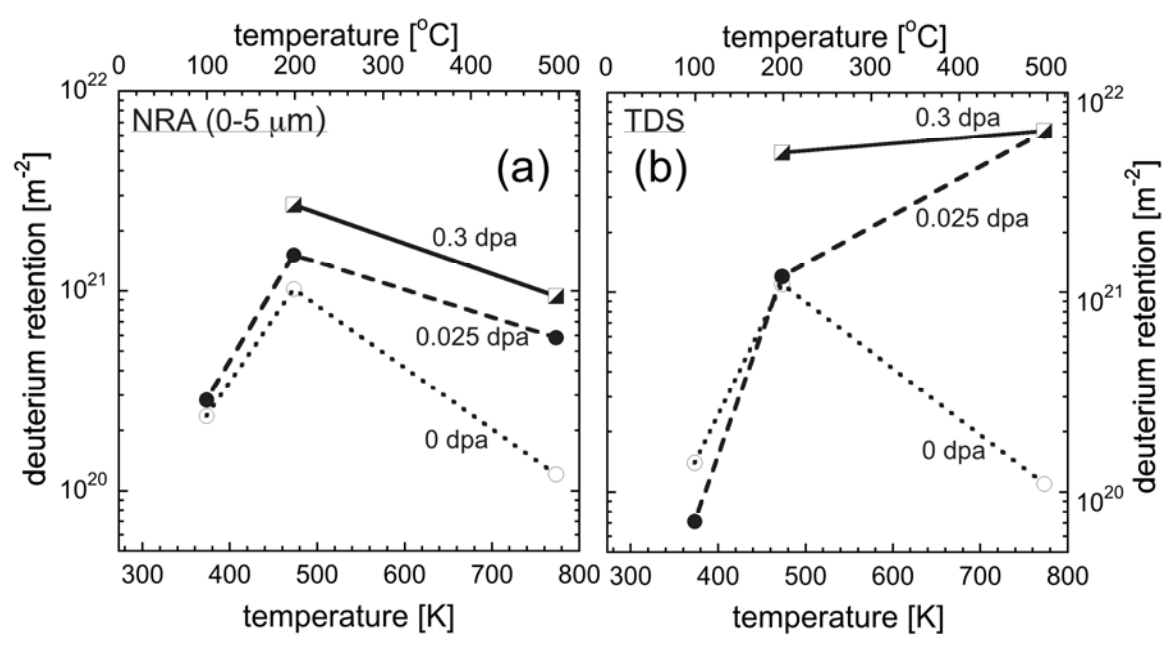


Figure 4. (a) Near-surface (0-5 μ m) deuterium retention and (b) total deuterium retention at three different plasma exposure temperatures (100, 200, and 500 °C).

[figure width: two column, black and white only, filename: "NF_MShimada_fig4.tif"]

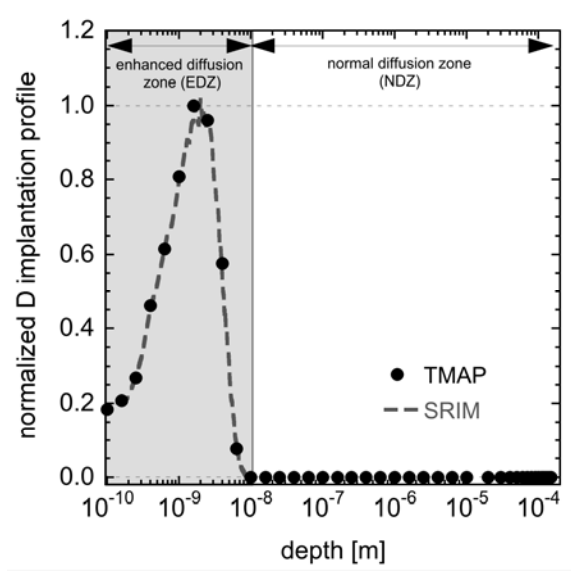


Figure 5. Deuterium ion implantation profile used in the TMAP simulation along with the profile obtained by SRIM code in entire sample thickness.

[figure width: one column, black and white only, filename: "NF_MShimada_fig5.tif"]

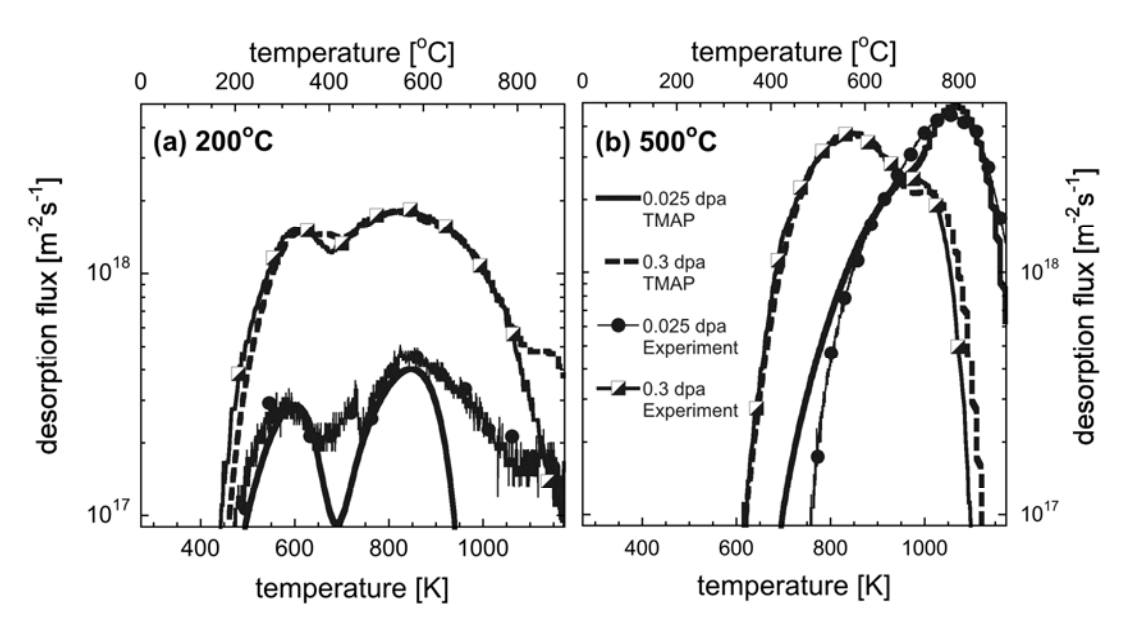


Figure 6. Tritium Migration Analysis Program (TMAP) modeling of thermal desorption spectra of 0.025, and 0.3 dpa neutron-irradiated tungsten samples exposed to the total ion fluence of 1×10^{26} m⁻² at (a) 200 °C and (b) 500 °C.

[figure width: two column, black and white only, filename: "NF_MShimada_fig6.tif"]

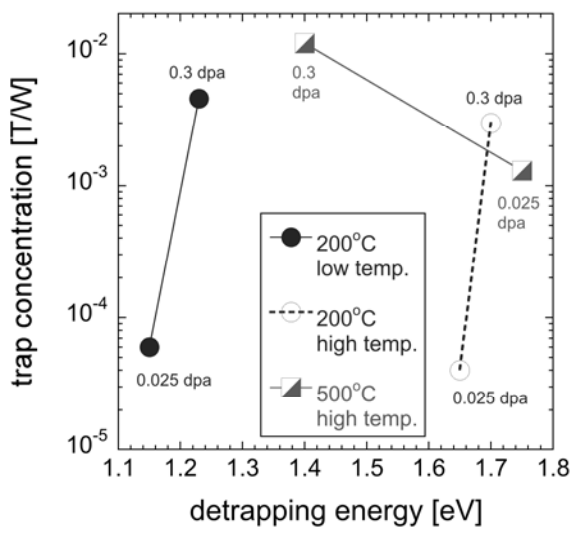


Figure 7. Detrapping energy and trap concentration of trap sites obtained from TMAP modeling on experimental TDS spectra of 0.025, and 0.3 dpa neutron-irradiated tungsten samples exposed to the total ion fluence of $1x10^{26}$ m⁻² at 200 °C and 500 °C. There exists roughly two TDS peaks for 200 °C (low temperature peak and high temperature peak), whereas there is only one TDS peak for 500 °C (high temperature peak).

[figure width: one column, black and white only, filename: "NF_MShimada_fig7.tif"]

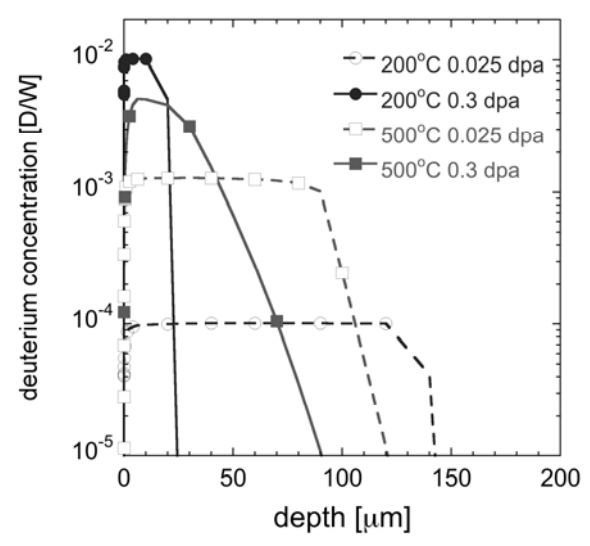


Figure 8. Deuterium depth profile obtained from TMAP modeling on experimental TDS spectra of 0.025, and 0.3 dpa neutron-irradiated tungsten samples exposed to the total ion fluence of 1×10^{26} m⁻² at 200 °C and 500 °C.

[figure width: two column, black and white only, filename: "NF_MShimada_fig8.tif"]